Growth, Structural, NLO and Impedance Properties of Cu2+ doped Lithium Sulphate Monohydrate Single Crystals

A Annalakshmi (anubala81@gmail.com)
Sri Paramakalyani College https://orcid.org/0000-0003-1205-2273
K. Balasubramanian
The MDT Hindu College, Tirunelveli

Research Article

Keywords: Single crystal, Atomic force microscopy, Impedance, AC conductivity, Modulus, Dielectric constant

Posted Date: March 22nd, 2021

DOI: https://doi.org/10.21203/rs.3.rs-328550/v1

Growth, Structural, NLO and Impedance Properties of Cu^{2+} doped Lithium Sulphate Monohydrate single crystals

A.Annalakshmi[1] (Reg. No: 11973), K. Balasubramanian[2]

[1]PG & Research Department of Physics, Sri Paramakalyani College, Alwarkurichi, 627 412, Tamilnadu, India

[2]PG & Research Department of Physics, The M.D.T. Hindu College, Tirunelveli, 627 010, Tamilnadu, India

([1,2]Affiliated to ManonmaniamSundaranar University, Abishekapatti, Tirunelveli, 627 012, Tamilnadu, India)

Abstract

Single crystals of 2.5 mole% of Cu^{2+} doped Lithium sulphate monohydrate (LSMH) have been grown using slow evaporation technique at room temperature. Powder X-ray diffraction (PXRD) analysis ensures that the crystal belongs to monoclinic crystal system. The variation of relative dielectric constant, dielectric loss and tangent loss with frequency have been discussed. The conductivity and dielectric relaxation mechanism involved in the grown crystals have been carried out by using complex impedance spectroscopy in the temperature range (343K and 353K) and in the frequency range from 20Hz to 2MHz. The frequency dependent ac conductivity obeys the Jonscher's power law. The imaginary part M″ of electrical modulus of grown crystals shows the formation of asymmetric dispersion peak and indicating non- Debye relaxation behaviour. Morphology properties of the grown crystals have been studied using atomic force microscopy and hence the roughness of the grown crystals has been calculated. The NLO property and LDT values of the grown crystals are analysed using Nd:YAG laser operating at 1064 nm and 532 nm respectively.

Keywords: Single crystal; Atomic force microscopy; Impedance; AC conductivity; Modulus; Dielectric constant

1. Introduction

In the recent past, the growth of non centro symmetric crystals with distinguishable and remarkable piezo electric, pyroelectric, ferroelectric and non linear optical properties have been used in various device fabrications focussed in the areas of telecommunication, optoelectronic industries etc., [1-3]. Nowadays it's a challenging endeavour to grow single crystals with high crystalline perfection. With respect to its structural and physical properties, LSMH is one of the promising materials among alkali metal sulphates. In addition to this, it is an efficient piezoelectric, pyroelectric and NLO material and exhibits good mechanical and thermal properties. Many studies have been reported that by adding low valence cation dopants to the inorganic crystals make many significant impact on its physicochemical and electrical properties.

There are some literatures focussed on growth and characterization of Cu^{2+} doped LSMH, Elucidation of site symmetry, location, bond, ground state of Cu^{2+} ions in lithium sulphate monohydrate single crystal through EPR and optical studies etc.,[4,5] In our earlier work we have also reported the effect of Cu^{2+} ions on linear optical properties of Undoped LSMH [6]. But least attention has been given to the study of conductivity and morphological properties of the title compound. When LSMH single crystals doped with divalent impurities, there may be formation of cation vacancies by the dopants which will affect the conductivity of the crystals. According to the Goldschmidt rule, free substitution of the dopant cation is possible only when the difference between the radius of the substituted ion and replaced ion must be less than 15%[7]. The dopant Cu^{2+}has been selected because ionic radii of Cu^{2+}ion (0.73Å) is nearer to that of Li^{+} (0.76Å).

The current paper reports the growth, structural, dielectric, electrical and morphological properties of Cu^{2+} doped Lithium Sulphate Monohydrate (LSMH). But the main goal of the present work is to analyse the conductivity and surface morphological properties of Cu^{2+} doped LSMH single crystals.

2. Experimental procedure

Single crystals of Cu^{2+} doped Lithium sulphate monohydrate (LSMH) were grown by slow evaporation technique. Saturated solution of LSMH containing 2.5 mole% of copper sulphate pentahydrate was made for growing these crystals. The solution was stirred well for 4 hours to attain homogeneity. After a period of 25 days good quality crystals of 2.5 mole% Cu^{2+} doped LSMH were harvested. The grown doped crystals are shown in Fig. 1. The salts Lithium sulphate monohydrate and copper sulphate pentahydrate used in the present study were of pure grade procured from Sigma Aldrich.

3. Results and Discussion

3.1 Powder XRD Analysis

X-ray diffraction studies are taken for the powdered sample Cu^{2+} doped LSMH with Cu Kα radiation of wavelength 1.5406Å in 2θ range between 10-60°. PXRD pattern of the doped crystal is represented in Fig.2. It is noted that the Cu^{2+}doped LSMH belongs to monoclinic crystal system with the space group $P2_1$. The XRD pattern of doped crystal agrees well with the XRD pattern of pure LSMH [8-10] i.e. there is no phase change happens during doping. Moreover, the incorporation of metal ions in LSMH lattice accounts for least variation in the lattice parameters values. With the help of JCPDS software the hklvalues of the doped crystal is indexed. The lattice parameters of the grown crystals are given below in the Table 1.

3.2 Impedance Spectroscopy:

In Impedance spectroscopy particularly Nyquist plots have been employed to identify the grain, grain boundary and grain electrode effects in grown crystals[11]. The Nyquist plots of 2.5 mole% Cu^{2+} doped LSMH obtained at 343K and 353K temperatures are shown in Fig. 3. Interestingly two depressed semicircles have been observed in the doped crystal which is in contrast to the Pure LSMH crystal. The first semicircle at higher frequency is due to grain (bulk) effect and the next one at intermediate frequency is due to grain boundary . The radii of the depressed semicircle decreases as there is an increase in temperature and its real axis intercept is shifted towards origin [12]. Negative temperature coefficient of resistance behaviour is observed in the crystal. It is observed that centre of the semicircular arcs are below the real axis indicating non- Debye dielectric relaxation [13,14] which is due to the heterogeneity in the crystal and distribution of relaxation time within the crystal.[15]

The understanding of the relaxation processes and space charge carriers in the crystals have been studied by varying real part of impedance Z′ with log frequency under different temperature and the observations are shown in Fig 4. It is observed that Z′ decreases with increasing frequency which indicates the increase in ac conductivity [16] of the crystals with increasing frequency. This plot is well matched with ac conductivity plot. In the same breath Z′ also decreases with an increase in temperature. It is keenly seen that the Z′ values merge with each other at higher frequency which is due to the release of space charge carriers.

Fig 5 shows variation of imaginary part of impedance (Z″) with log frequency under different temperature. From fig 5 it is observed that at the low frequency region Z″ increases with the increase in frequency. Then two peaks are appeared at the intermediate and higher frequency region respectively. By increasing the temperature, the observed peaks are shifted towards higher frequencies and the curves are broadened with reduced peak height.

This asymmetric broadening suggests that the relaxation process in the grown crystal may be thermally active. This may be due to existence of immobile ions at lower temperature and defects at higher temperature. [17]

3.3 Modulus studies:

Modulus studies have been used in the crystal to understand their electrical transport phenomenon in the crystals. Electric modulus is defined by

$M^* = M' + jM''$ ---------- (1)

Where M′ is real part of modulus which contributes the capacity of the material to store energy. Argand plot for grown crystals at temperatures 343K and 353K is shown in Fig 6. The presence of depressed semicircles in the Argand plot confirms its deviation from ideal Debye behaviour.[18,19]

The frequency dependent real part of modulus M′ for grown crystals at temperatures 343K and 353K is shown in Fig 7. From Fig 7, it is noticed that by varying frequency from lower to higher value M′ exhibits step like increase and it attains almost constant value at higher frequency side for different temperatures. At low frequency region, the minimum value of M′ [20] is observed due to suppression of electrode polarization. In addition, the appearance of long tail at lower frequencies narrates the acquirement of large amount of capacitance value in the doped crystals. Then it exhibits steady increase in dispersion and attains saturate asymptotic value in the higher frequency region. By increasing the temperature, the values of M′ get decreased and the peaks get shifted towards higher frequency region.

The similar behaviour has been noticed in imaginary part of modulus (M″). High frequency curve in Fig 8 may be attributed to bulk properties of the grown crystals. Another conclusion can be drawn from M″ plot that the height of the peaks at higher frequencies changes with temperature. The reason behind is due to hopping of charge carriers. In addition to that the asymmetric and broad nature of peaks observed in M″ plot indicates the occurring of multiple relaxation times. In addition it also exhibits Non- Debye relaxation mechanism [21].

3.4 Frequency dependent ionic conductivity

Fig. 6 shows the variation of conductivity of the grown crystals as a function of frequency at various temperatures. Generally frequency dependent conductivity consists of three different regions, (i) a low frequency dispersive region corresponds to electrode polarization (ii) an intermediate frequency plateau region ascribed to Macroscopic dc conductivity of the crystals which is frequency independent and (iii) a high frequency dispersion region attributes to movement of ions which are frequency dependent whereas 2.5 mole% of Cu^{2+} doped LSMH crystals have only two region. The conductivity at low frequency region occurs due to accumulation of more charges at electrode-electrolyte interface [22]. At the mid frequency region, the conductivity increases with increasing temperature[23]. This behaviour indicates that the conductivities in the crystals are thermally active.

Hopping of ions takes place when the frequency is less than the hopping frequency (ω_p). Above the hopping frequency the conductivity increases with increase in frequency. The switch-over behaviour from frequency independent conductivity to dispersion conductivity shows that the relaxation mechanism is happening [24]. The conductivity in the grown crystal obeys Jonscher's power law [25]

$$\sigma_{ac} = \sigma_{dc} + A\omega^n \quad (2)$$

where σ_{dc} is the frequency independent dc conductivity, A is the pre-exponential constant, ω is the angular frequency and n is the power law exponent.

3.5 Dielectric studies:

The storing of electrical energy property in dielectric materials can be estimated by measuring its permittivity. Usually, the relative permittivity exhibits complex behaviour [26] in alternating electric fields. The real and imaginary part of dielectric permittivity are calculated from impedance data from the relation

$$\varepsilon' = \frac{Z''}{\omega C_0 (Z'^2 + Z''^2)} \quad \text{_____(3)}$$

$$\varepsilon'' = \frac{Z'}{\omega C_0 (Z'^2 + Z''^2)} \quad \text{_____(4)}$$

$$\tan\delta = \quad \text{_____(5)}$$

where Z' and Z'' are the real and imaginary parts of the impedance and C_0 is the vacuum capacitance and is given by $\frac{\varepsilon_o A}{d}$ where $\varepsilon_0 = 8.85\times10^{-12} Fm^{-1}$ is the permittivity of free space, A and dare the active area of the electrolyte and the thickness of the sample, respectively. The angular frequency is $\omega = 2\pi f$, where f is the frequency of the applied electric field.

Fig 10 exhibits the variation of dielectric constant, dielectric loss and loss factor as a function of frequency respectively. High magnitude of dielectric constant and dielectric loss is observed for the grown crystals at low frequency region which is due to contribution of charges at the surface of the electrode. Moreover at this region dipoles get aligned themselves along the direction of slow reversal applied ac field [27]. While at higher frequency region, the dipoles of the grown crystals are unable to align themselves in the direction of alternating field because of short time period of reversal AC field. Therefore ε' decreases rapidly and reaches close to zero at higher frequency region. This is the typical behaviour of polar dielectrics [28]. The dielectric loss (ε'') is also known as dissipation energy which means amount of energy loss in terms of heat.

Dielectric loss of the grown crystals follows the similar behaviour as dielectric constant. Large value of ε″ is obtained at lower frequency region due to movement of free charges within the crystals and interfacial polarization [29,30]. and decreases with increase in frequency.

From Fig 10 it is also concluded that ε″ increases with the increase in temperature. The variation of dielectric loss and loss factor with respect to the frequency and temperature can be explained with the help of Wagner theory [31]. According to the theory the dielectric material is composed of conducting grains and highly insulated grain boundaries which results in accumulation of charge at interfaces, giving rise to large dielectric and polarization values in the frequency range up to ~10^4 Hz. Apart from frequency and temperature , the size, shape and orientation of the conducting grains have an effect on the dielectric loss. The loss factor is directly proportional to the percentage of volume of the grains. If all the grains present in the crystal have the same conductivity a sharp maximum peak is observed at a particular frequency [32]. The loss factor also gives information on the relaxation mechanism of the crystals.

3.6 Atomic force microscopy studies

AFM images have been recorded to study surface morphological behaviour. Fig 11 A and B show two and three dimensional topographical images of the grown crystals respectively in contact mode within the scan area of 5µm x 5µm at room temperature.

Some smooth surface and small pores have been observed in the two dimensional image of the grown crystal. A well defined mountains and valleys have been observed in the three dimensional topography images of the grown crystal [33]. The maximum roughness height obtained in the grown crystal is 125.6nm. The root mean square (rms) roughness values are found to be 65nm.

3.7 NLO Test

With the aid of Kurtz and Perry powder technique, the NLO property of the grown crystal was analysed [34]. The grown crystal was first powdered and then it was irradiated by Nd: YAG laser of 1064 nm, light of 9 ns pulses and with the input laser of energy 850 mJ. The SHG property of the grown crystal is confirmed by the emission of green light at 532nm and its SHG efficiency is 1.1 times than that of KDP crystal (well-known reference material).

3.8 LDT studies

The laser damage threshold measurement was done on grown crystal using a Q switched Nd: YAG laser for 6 ns laser pulses. Usually, threshold was determined by dislocations in the crystal. Laser damage

threshold value will be higher for perfect crystalline crystals. Therefore crystals with many dislocations will have low damage threshold. The surface damage threshold of the crystals were calculated by the formula

Power density, $P_d = E/\pi r^2\tau$ ---------- (6)

Where E is the laser energy in mJ, r is the radius of the beam in cm and τ is the pulse width in ns of the laser. The calculated LDT value for the grown crystal is 0.32 GW/cm^2

4. Conclusion

By adapting the method of slow evaporation, single crystals of 2.5 mole% of Cu^{2+} doped LSMH are obtained. The presence of grains and grain boundaries in the crystal are analysed using complex impedance spectroscopy (CIS). Furthermore, Negative temperature coefficient of resistance (NTCR) behaviour and the relaxation mechanism involved in the grown crystal has been explained.The frequency dependent conductivity has been interpreted by using Jonschers power law. It is also observed that the dielectric constant, dielectric loss and loss factor of grown crystals increase with temperatureand decrease sharply with increase in frequency. The 2D and 3D topographical images of grown crystal is shown and its roughness is calculated. The SHG efficiency of the grown crystal is found to be greater than that of KDP. Laser damage threshold value for doped crystal is calculated.

References

[1] Ch. Bosshard, K. Sutter, R. Schlesser, P. Gunter, Electro-optic effects in molecular crystals, J. Opt. Soc. Am. B: Opt. Phys. 10 (1993) 867–885.

[2] R.F. Belt, G. Gashurov, Y.S.Liu, KTP as a harmonic generator for Nd:YAG lasers, Laser Focus 21 (1985) 110.

[3] R.H. Bube, Photoconductivity of Solids, John Wiley, New York, NY, 1960.

[4] K. Boopathi, P. Ramasamy, G. Bhagavannarayana, J. Cryst. Growth, 2014, 386, 32–37.

[5] P.Subramanian, K.Julietsheela, S.Radha Krishnan, V.M.Shanmugam,Journal of Molecular Structure, 2020, 1206,127586

[6] A.Annalaksmi and K.Balasubramanian: IOSR- JAP, 2017, 19-25, 2278-4861.

[7] Masaki Takahashi, Norihisa Hoshino, KoheiSambe, Takashi Takeda, Tomoyuki Akutagawa. Inorganic Chemistry **2020,** 59 (16), 11606-11615.

[8] A.Annalaksmi and K.Balasubramanian: JOICS, 2020, 10(5), 307-328, 1548-7741.

[9] N.W. Alcock, D.A. Evans, H.D.B. Jenkins, ActaCrystallogr. B 29, 360 (1973)

[10] Rama Rao, S., Bheema Lingam, C., Rajesh, D., Vijayalakshmi, R. P., &Sunandana, C. S. (2014).Eur. Phys. J. Appl. Phys. (2014) 66: 30906

[11] J. R. Macdonald, Impedance Spectroscopy Emphasizing Solid State Materials (John Wiley & Sons, Inc., New York, 1987).

[12] Barranco AP, Pinar FC, Martínez OP, et al. J Eur Ceram Soc 1999, 19: 2677–2683.

[13] B. Behera, P. Nayak, and R. N. P. Choudhary, Mater. Chem. Phys. 106, 193 (2007).

[14] D. K. Pradhan, R. N. P. Choudhary, C. Rinaldi, and R. S. Katiyar, J. Appl. Phys. 106, 024102 (2009).

[15] Suman, C.K.; Prasad, K.; Choudhary, R.N.P. Indian Journal of Engineering & Materials Sciences, 2008, 15, 157-162.

[16] Barde, R.V.; Nemade, R.K.; Waghuley, S.A. Journal of Asian Ceramic Societies, 2015, 3, 116-122. DOI:10.1016/j.jascer.2014.11.006

[17] Bharadwaj SSN, Victor P, Venkateswarulu P, et al. Phys Rev B 2002, 65: 174106.

[18] Singh, H., Kumar, A., Yadav, K.L.: Mater. Sci. Eng. 176, 540–547 (2011)

[19] Behera, B., Nayak, P., Choudhary, R.N.P.: Mater. Chem. Phys. 106, 193–197 (2007)

[20] Das, P.R., Pati, B., Sutar, B.C., Choudhary, R.N.P.: Adv. Mat. Lett. 3, 8–14 (2012)

[21] Y. Lin, H. Yang, and Z. Zhu, Mater. Chem. Phys. 136, 286 (2012)

[22] Satiner M, Charles Hardy L, Whitmore DH, Shriver DF (1984). J Electrochem Soc 131:784–790

[23] T. Kikuchi, A. Watanabe, K. Uchida, Mater. Res. Bull. 12 (1997) 299.

[24] R.E. Newnham, R.W. Wolfe, J.F. Dorrian, Mater. Res. Bull. 6 (1991) 1029

[25] A. K. Jonscher, Nature 267, 673 (1977).

[26] A. Srinivas, S.V. Suryanarayana, G.S. Kumar, M. Mahesh Kumar, J. Phys.: Condens. Matter 11 (1999) 3335.

[27] A. Chen, Y. Zhi, L.E. Cross, Phy. Rev. B 62 (2000) 228.

[28] Singh, N.K.;Kumar, P.; Kumar, A.; Sharma, S. Journal of Engineering and Technology Research, 2012, 4(6), 104-113. DOI: 10.5897/ JETR12.002

[29] Jianjun, L.; Duan, CG.;Yin, WG.; Mei, W.N.; Smith R.W.; Hardy, John R. Physical Review B. 2004, 70, 144106(1-7). DOI: 10.1103/ PhysRevB.70.144106

[30] Nishizaki, S.; Kusakawa, H.; *Bull. Chem. Soc. Jpn.* 1963*, 36*, 1681-1683.

[31] Singh, R.A.; Singh, V,K.; 1997. *Bull. Mater. Sci.* 1997*, 20(3),* 305-315.

[32] Akamatu, H.; Inokuchi, H.; Matsunaga, Y. *Nature*, 1954,*173*, 168-169. DOI:10.1038/173168a0

[33] Mendez-Vilas A and Diaz J (eds) 2007 Modern research andeducational topics in microscopy (Badajoz: FORMATEX) vol. 2

[34] S.K. Kurtz, T.T. Perry, Journal of Applied Physics 1968, 44, 455.

Figures

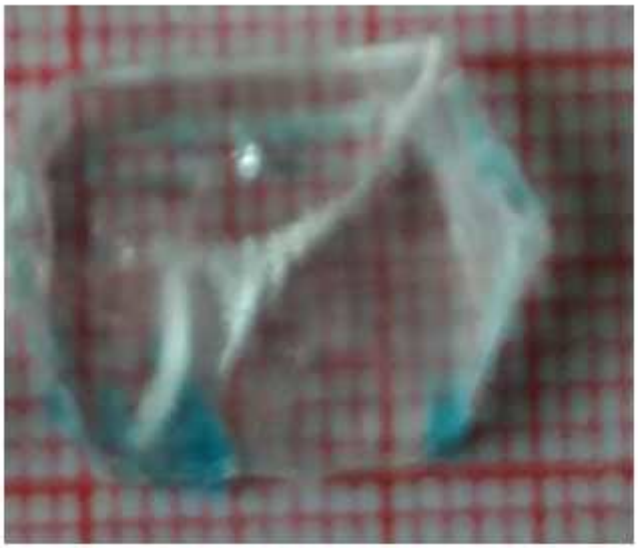

Figure 1

Photograph of Cu2+ doped LSMH

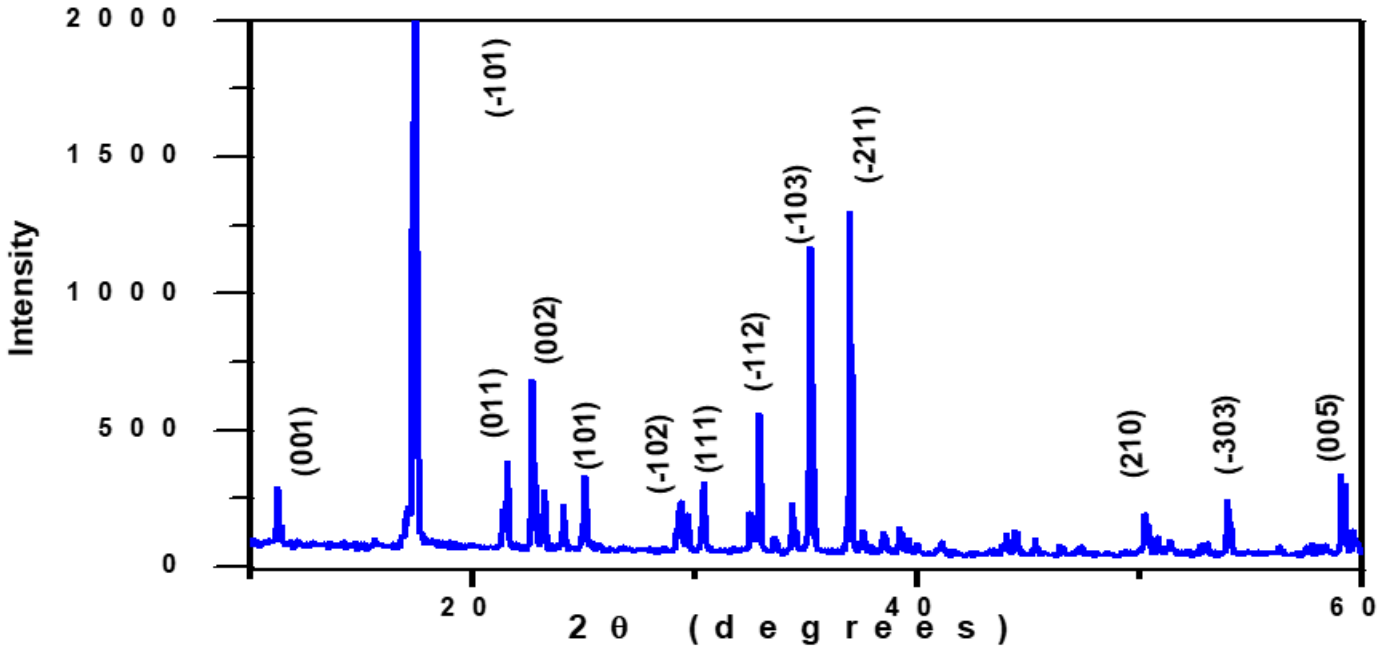

Figure 2

PXRD pattern of Cu2+doped crystal

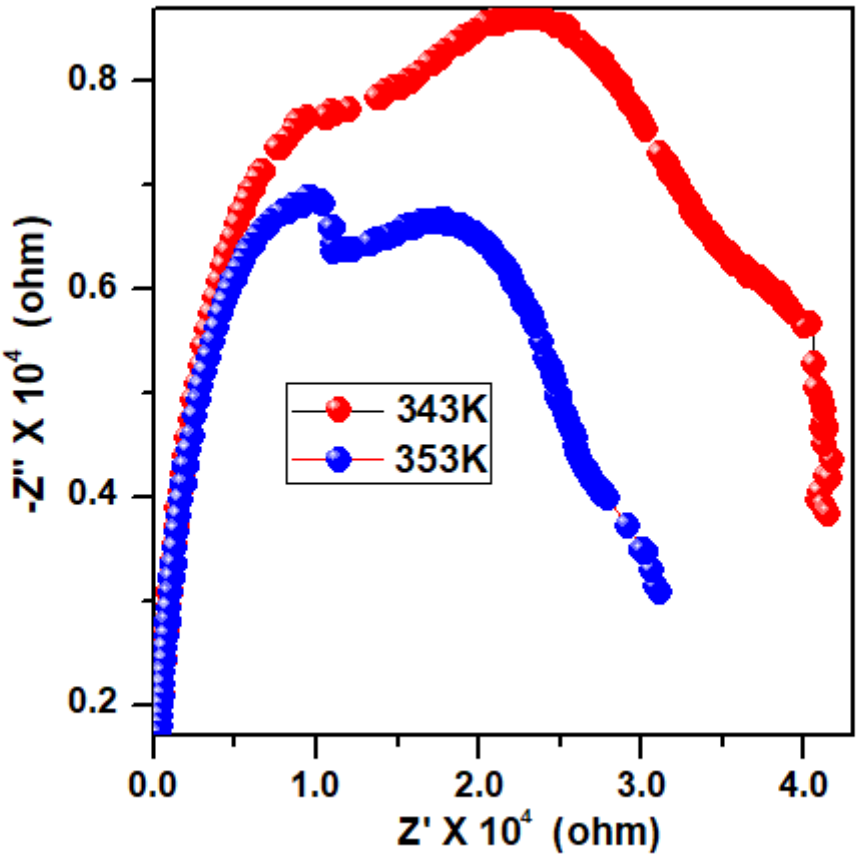

Figure 3

Complex impedance spectra of Cu2+doped crystal

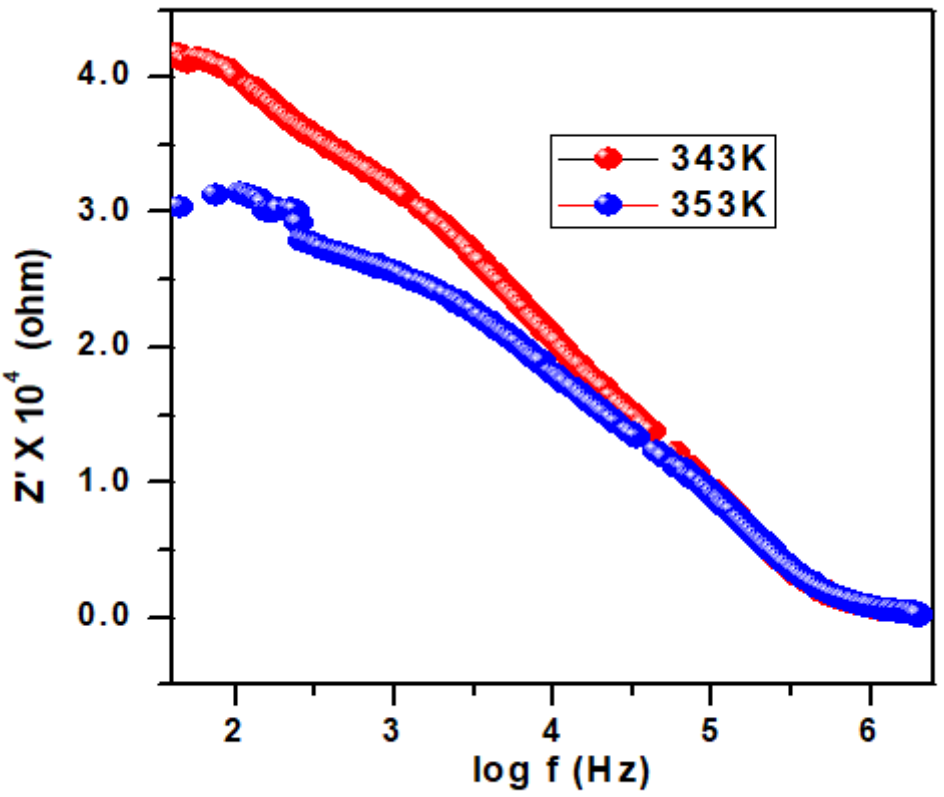

Figure 4

Variation of real part of impedance of Cu2+doped crystal

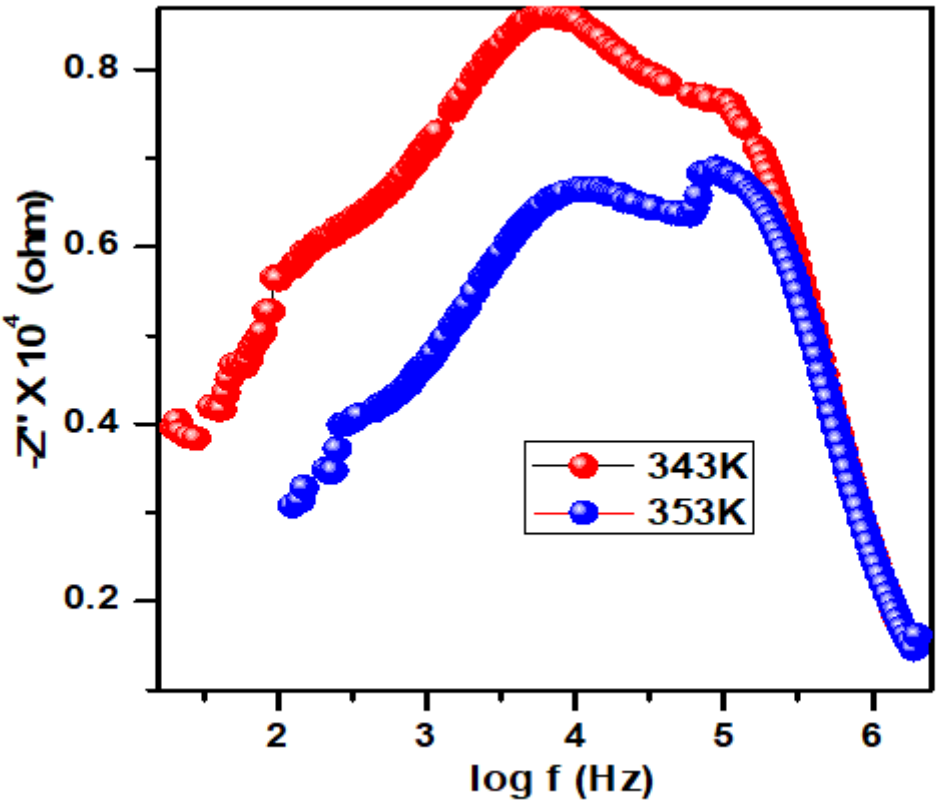

Figure 5

Variation of Z” Vs log f of Cu2+doped crystal

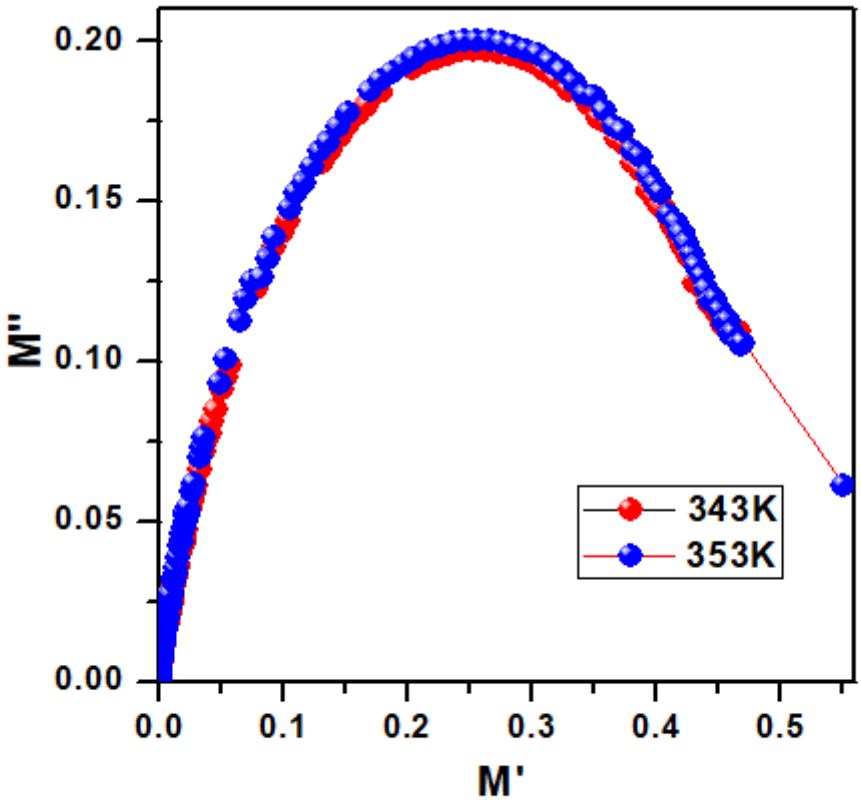

Figure 6

Argand plot of Cu2+doped crystal

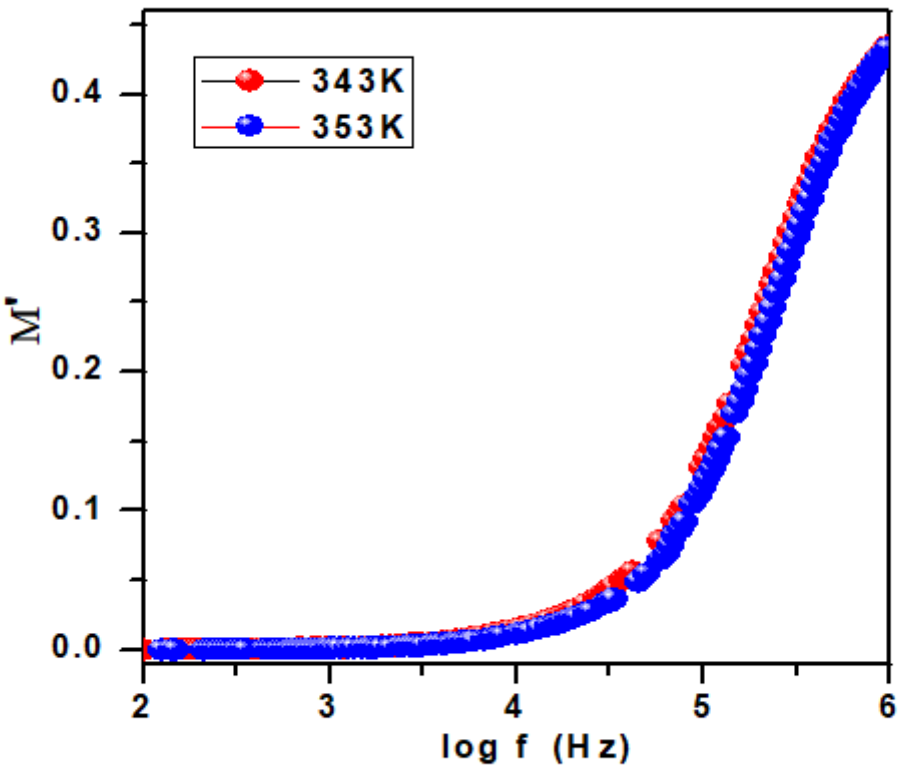

Figure 7

Variation of real part of modulus as a function of frequency of Cu2+doped crystal

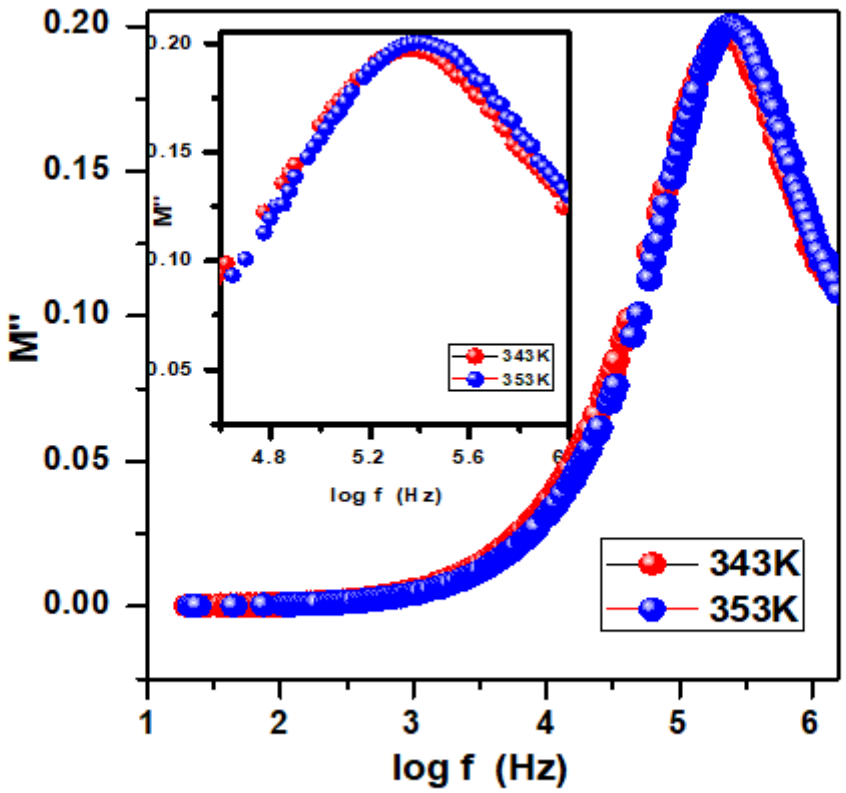

Figure 8

Variation of imaginary part of modulus as a function of frequency of Cu2+doped crystal

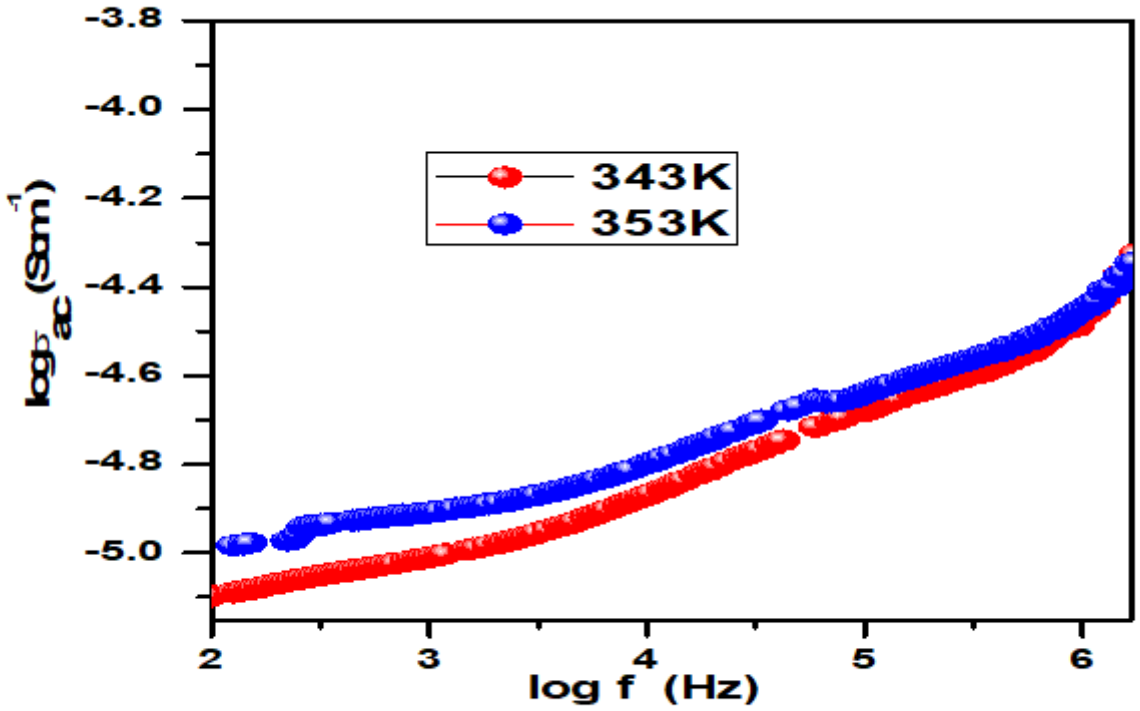

Figure 9

Frequency dependent Ac conductivity of Cu2+doped crystal

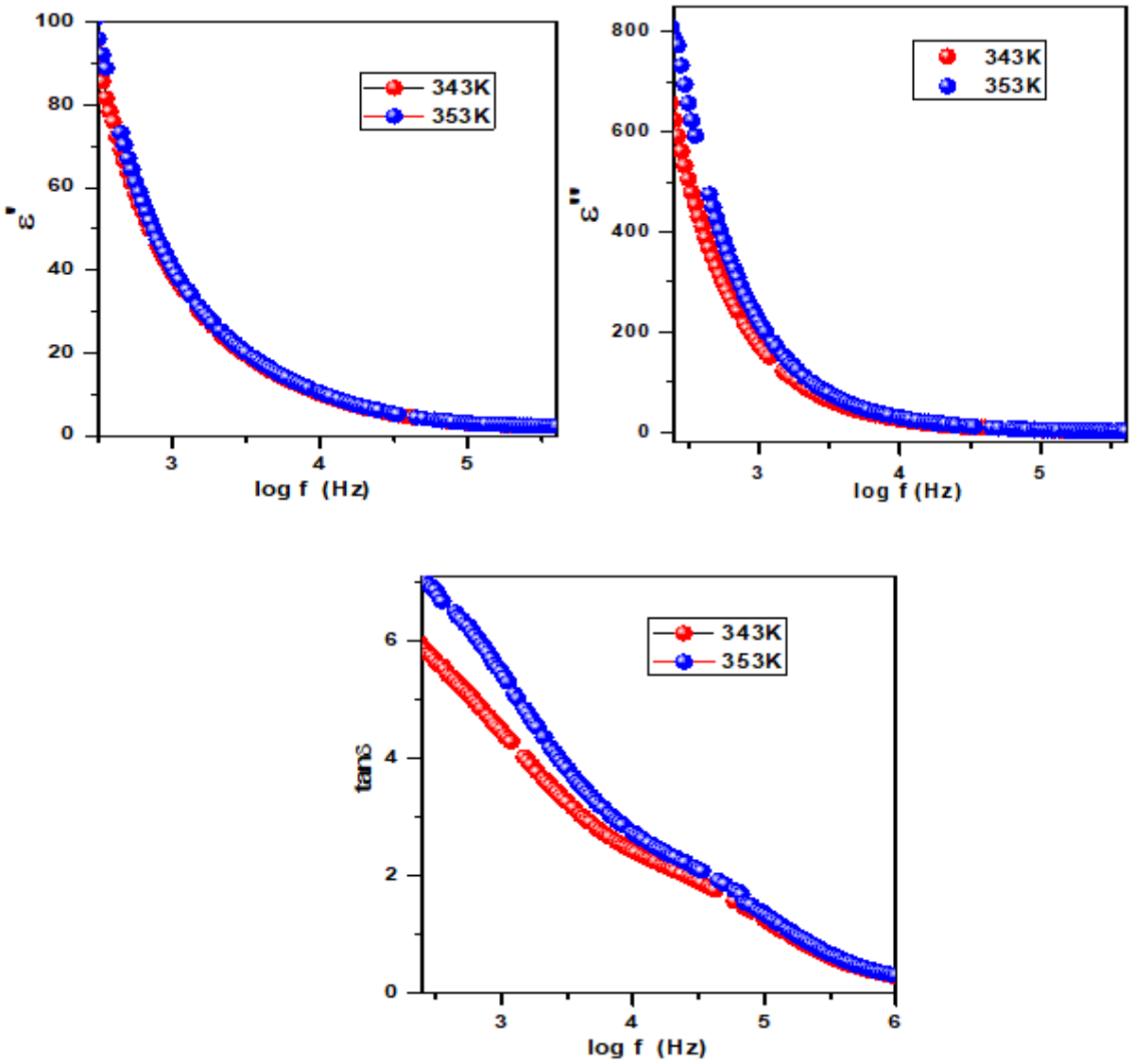

Figure 10

Variation of ε′, ε″ and loss factor with log f for grown crystals

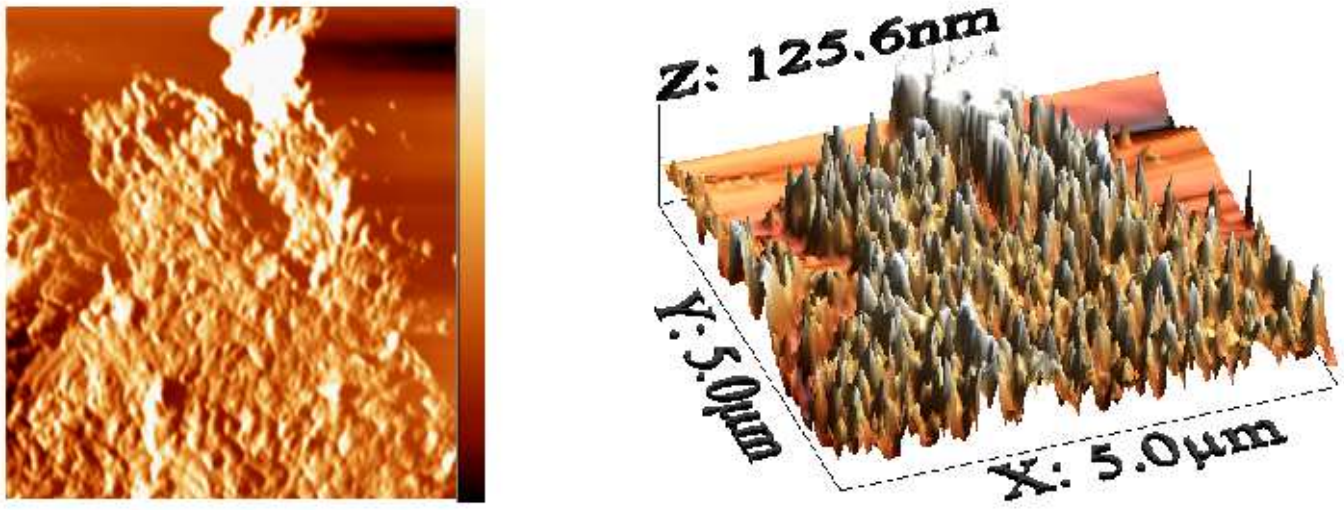

Figure 11

A) 2D topographical image B) 3D topographical image